TECHNICAL NOTE

Quick MR Neuromelanin Imaging Using a Chemical Shift Selective Pulse

Midori Kusama, Noriko Sato[*], Yukio Kimura, and Kenji Miyagi

Not only magnetization transfer contrast (MTC) pulse, but also chemical shift selective (CHESS) pulse would be a useful additional one for shortening the scan time of neuromelanin imaging. We compared three sequences among turbo-spin echo (TSE) images with CHESS, MTC, and without an additional pulse in the same short time, 3 min 20 s. The TSE with CHESS image was the most useful for the diagnosis of neuromelanin within the limited time.

Introduction

Sasaki et al.[1] described neuromelanin imaging that used the T_1-weighted turbo spin-echo (TSE) method optimized for detecting the melanin of the locus coeruleus (LC) and the substantia nigra pars compacta (SNc) as a high signal in 2006. This imaging method has enhanced the usefulness of MRI-based diagnoses of alpha synuclenopathies such as Parkinson's disease. Only high-field tesla (T) MR allows this imaging, and it was first established after 3T MR emerged. In addition to the high signal-to-noise ratio (SNR) of 3T, the T_1 lengthening, the increased number of excitations, and the off-resonance frequency component included in the 180° pulse of TSE suppressing the brain parenchymal signal enabled neuromelanin imaging. However, a problem with neuromelanin imaging is that it takes a long time, i.e., approx. 12 min.

Ogisu et al.[2] reported that good contrast of neuromelanin can be obtained by using a magnetization transfer contrast (MTC) pulse in a three-dimensional gradient recalled echo (3D-GRE) sequence in 3T-MRI. This is because the magnetization transfer (MT) effect, which is one of the factors that enable neuromelanin images, provides a high contrast between background tissue and neuromelanin. Generally, in order to obtain the MT effect, an MTC pulse—which is a radiofrequency (RF) pulse of a frequency component far from the free water resonance frequency—is applied. Similarly, there is a report that the use of a frequency-selective fat suppression [i.e., chemical shift selective (CHESS)] pulse applying an RF pulse as the presaturation pulse also has the MT effect.[3]

We conducted this study to examine the appropriate imaging method that can be used in the shortest possible time for neuromelanin imaging in daily clinical practice. We set the imaging time at 3 min 20 s, which would be feasible in clinical practice. The scan time was shortened by decreasing the in-plane resolution, and the number of additions. Instead of these full values, we added MTC or CHESS to cover the neuromelanin contrast. We used the 2D-TSE method instead of the 3D-GRE sequence to reduce the imaging time, taking into account the rise in the specific absorption rate (SAR) and longer scan times. We qualitatively and quantitatively compared three types of imaging methods (TSE alone, MTC pulse application, and CHESS pulse application) using the same scan time with respect to visualization of the neuromelanin of the SNc and LC.

Participants and Methods

Participants

Thirty-one healthy volunteers (12 males and 19 females aged 26–59 years, average age 47 years) participated. None had a history of neurological or psychiatric illness, and no abnormalities were observed on their brain MR images. All participants gave written consent to participate in the study, which was approved by the Institutional Review Board at the National Center of Neurology and Psychiatry, Japan.

Imaging acquisition

MR images of the subjects were acquired using a 3T MR scanner (MAGNETOM Verio, Siemens Medical Solutions, Erlangen, Germany) with a 32-channel head coil. Three sequences were scanned on each subject: axial T_1-weighted TSE with CHESS (hereafter referred to as 'CHESS'); T_1-weighted TSE with MTC ('MTC'); and T_1-weighted TSE without CHESS or MTC ('TSE').

Department of Radiology, National Center of Neurology and Psychiatry, Tokyo, Japan

[*]Corresponding author: Department of Radiology, National Center of Neurology and Psychiatry, 4-1-1 Ogawa-Higashi, Kodaira, Tokyo 187-0031, Japan. Phone: +81-42-341-2711, Fax: +81-42-344-6745, E-mail: snoriko@ncnp.go.jp

The T_1-weighted TSE images were obtained using the following settings: 600/10 repetition time/effective echo time (TR/TE); 3-echo train length; 3-mm section thickness with 0.6-mm intersection gaps; 16 slices; matrix size 192 × 163; and 130-mm field of view (FOV; pixel size 0.80 × 0.68 mm). The acquisition time in all three sequences was 3 min 20 s.

Chemical shift selective

There is a 3.5-ppm difference in resonance frequency (chemical shift) between fat and water. The CHESS method selectively saturates the fat signal by adding a narrow bandwidth prepulse to only the fat resonance frequency.[4] In the CHESS method, the whole FOV is irradiated with a 90° RF saturation pulse of the fat resonance frequency to suppress the signal from the fat.[5] Since the imaging sequence is started immediately after the CHESS pulse, the longitudinal magnetization of the fat has no time to recover, and the signal of the fat is suppressed. Shortly thereafter, a spoiler pulse is also applied to completely erase the transverse magnetization. This pulse accelerates the relaxation of fat and erases the remaining transverse magnetization.[6]

Magnetization transfer contrast

Magnetization transfer contrast imaging is a method of indirectly suppressing the proton signal of free water by saturating protons of bound water with the use of an RF pulse. Protons in the living body exist in various forms such as free water protons that can move freely, protons of bound water, and protons bound to macromolecules such as proteins that are restricted in movement. Because the protons that are bound to macromolecules have a very short T_2 value, the transverse magnetization quickly decays and is not detected as a signal in conventional MRI. On the other hand, protons of free and bound water move freely back and forth (chemical exchange), and a transfer of magnetization takes place between them. This can affect the MR signal.

The protons in the bound water have a wide-ranging resonance frequency. In contrast, free water has a narrow resonance frequency range. To saturate the bound water proton signals, an RF pulse with a narrow frequency range is irradiated at several to several tens of Hz away from the resonance frequency of free water protons. This RF pulse induces a chemical exchange between free and bound water protons, and a part of the saturated bound water portion moves to free water protons. As a result, the signal from free water protons is reduced. This phenomenon is called saturation shift, and the images obtained by this method are called MTC images.[7]

Data analyses
Qualitative assessment

Two neuroradiologists (N.S. and Y.K. with 26 and 14 years of experience, respectively) independently visually assessed the contrast of the SNc and LC in the CHESS, MTC, and TSE images and scored them according to the following three-point scale: 3, good; 2, moderate; and 1, poor. 'Good' means normal view of the SNc and the LC with high signal intensity bilaterally and no volume loss, indicating a healthy SNc and the LC, and 'moderate' means possible abnormality with reduced signal or volume of the SNc and the LC unilaterally or bilaterally. 'Poor' is definite abnormality with reduced signal or volume of the SNc and the LC (Figs. 1 and 2).[8] The two neuroradiologists solved any disagreements by a consensus reading of images. Their consensus grading scores were used in the analyses of the SNc and LC in the CHESS, MTC, and TSE images.

Quantitative assessment

The signal intensities of the SNc and LC were calculated on a liquid crystal display with the U.S. National Institutes of Health software platform ImageJ. Each section was set to an oblique axis direction perpendicular to the anterior commissure-posterior commissure line. In each of the CHESS, MTC, and TSE images, the signal intensity was measured by manually drawing the left and right SNc at the section through the inferior edge of the inferior colliculus. The data of each side were averaged.

The mid-portion of the adjacent superior cerebellar peduncle was measured twice, using 13-mm^2 round cursors, and these values were averaged.[9–14] The signal intensity of the LC was measured at 7 mm below the section through the inferior edge of the inferior colliculus, where the signal was most evident. The signal intensity of the LC and that of the midportion of the adjacent pontine tegmentum were measured using 1.5-mm^2 round cursors and 9-mm^2 oval cursors, respectively. The values of the right and left LC were
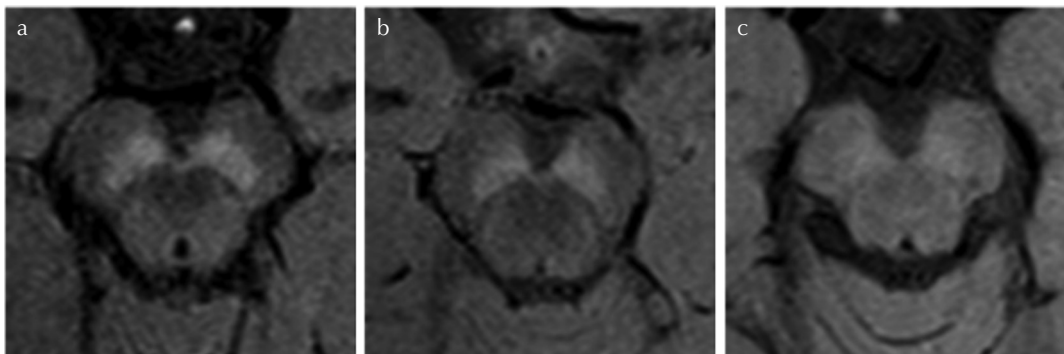
Fig. 1 Examples of the three-point scale for the contrast of the substantia nigra pars compacta (SNc) by visual assessment. (**a**) Grade 1 (good): MTC image. (**b**) Grade 2 (moderate): MTC image. (**c**) Grade 3 (poor): TSE image. MTC, magnetization transfer contrast; TSE, turbo spin-echo.

averaged.[15] The values of the mid-portion of the adjacent pontine tegmentum were measured twice, and the average of the two values was used.[9,12,14–16]

The contrast ratio of the SNc was calculated as $CR_{SN} = (S_{SN}–S_{SCP})/S_{SCP}$, where S_{SN} and S_{SCP} denote the signal intensities of the SNc and superior cerebellar peduncle, respectively. The contrast ratio of the LC was calculated as $CR_{LC} = (S_{LC}–S_{PT})/S_{PT}$, where S_{LC} represents the signal intensity of the LC, and S_{PT} represents that of the pontine tegmentum.

Statistical analyses
In the qualitative assessment, the comparison of the CHESS, MTC, and TSE images was performed using the Friedman test. The significance level of the post-hoc test was determined with a Bonferroni correction. A *P*-value < 0.05 was considered significant. The inter-observer reliability of the visual assessments was determined by using the weighted kappa (κ) statistic, after the independent assessments by the two neuroradiologists. The inter-observer agreement for the visual assessment was calculated as a κ-value. The strength of agreement was considered fair for κ-values of 0.21–0.40, moderate for κ-values of 0.41–0.60, good for κ-values of 0.61–0.80, and excellent for κ-values of ≥ 0.81.

In the quantitative analysis, we evaluated the differences in the CR_{SN} and CR_{LC} values among the CHESS, MTC, and TSE images by conducting a one-way repeated-measures analysis of variance (ANOVA), followed by a Bonferroni's correction. The data are expressed as the mean ± standard deviation. A *P*-value < 0.05 was considered significant. The statistical analyses were performed using SPSS (ver. 25.0, SPSS Tokyo, Japan).

Results

Qualitative visual analysis results
The κ-values for the inter-observer variability between the two reviewers for the evaluation of the SNc and the LC were 0.723 and 0.714, respectively for the CHESS images. For the MTC images, the corresponding values were 0.709 and 0.668, and in the TSE images, they were 0.704 and 0.655.

In the visual assessment of the SNc, there were no significant differences between the CHESS and MTC images (*P* = 1.00). The scores of the CHESS and MTC images were significantly higher than those of the TSE images (*P* < 0.001 and *P* < 0.001, respectively) (Fig. 3). In the visual assessment of the LC, the scores of the CHESS images were significantly higher than those of the MTC and TSE images (*P* = 0.021 and *P* < 0.001, respectively) (Fig. 4). There were no significant differences between the MTC and TSE images (*P* = 0.199).
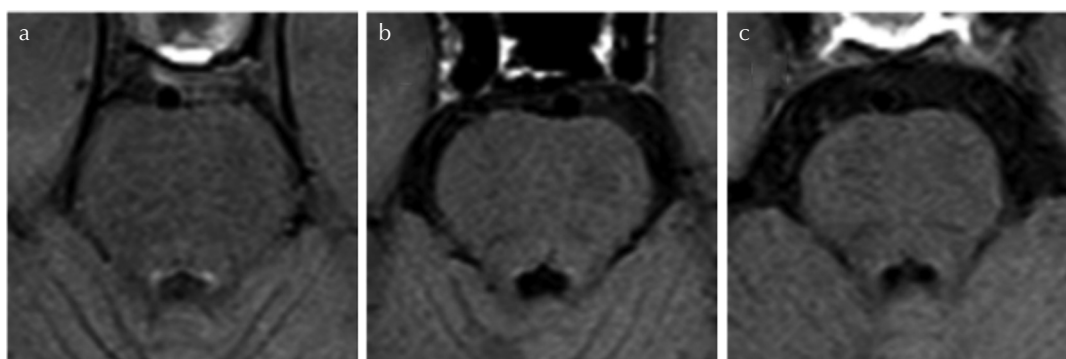

Fig. 2 Examples of the three-point scale for the contrast of the locus coeruleus (LC) by visual assessment. (**a**) Grade 1 (good): CHESS image. (**b**) Grade 2 (moderate): TSE image. (**c**) Grade 3 (poor): TSE image. CHESS, chemical shift selective; TSE, turbo spin-echo.
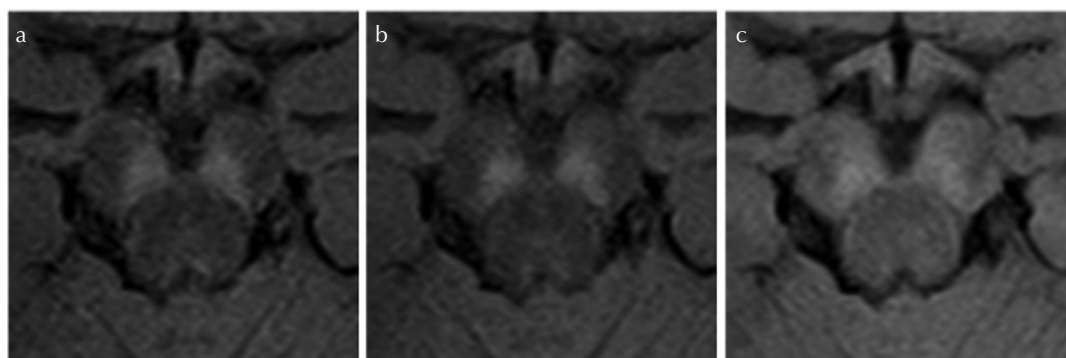
Fig. 3 Visual assessment of the contrast of the SNc compared with the background in the same subject. (**a**) CHESS image, (**b**) MTC image, (**c**) TSE image. Both the CHESS and MTC images show good contrast (Grade 1), which is better than the TSE image (Grade 2). SNc, substantia nigra pars compacta; CHESS, chemical shift selective; MTC, magnetization transfer contrast; TSE, turbo spin-echo.
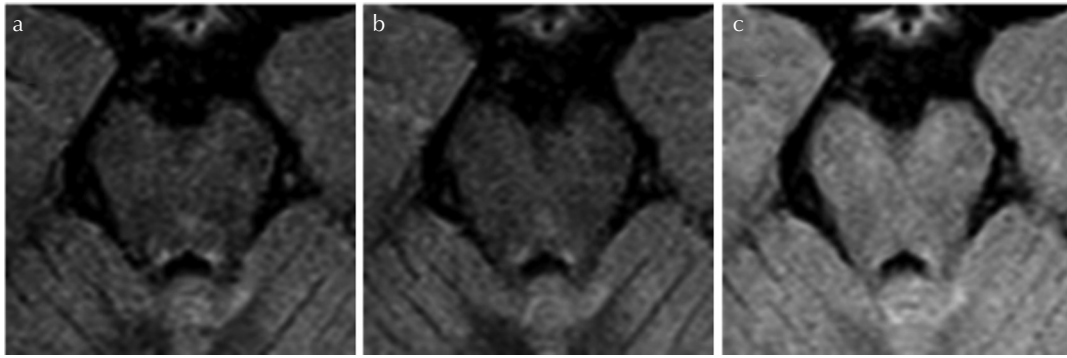
Fig. 4 Visual assessment of the contrast of the LC compared with the background in the same subject. (**a**) CHESS image, (**b**) MTC image, (**c**) TSE image. The CHESS image shows good contrast (Grade 1), better than the MTC and TSE images. The MTC image shows moderate contrast (Grade 2), which is better than the TSE image (Grade 3). CHESS, chemical shift selective; MTC, magnetization transfer contrast; TSE, turbo spin-echo; LC, locus coeruleus.
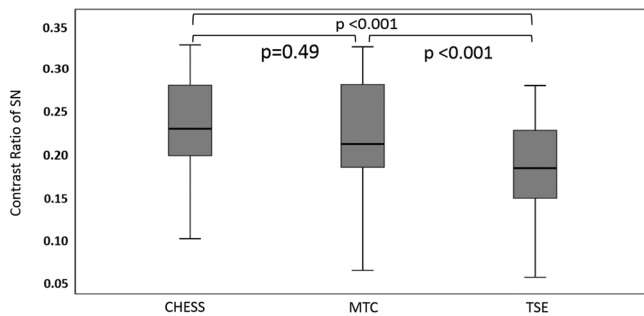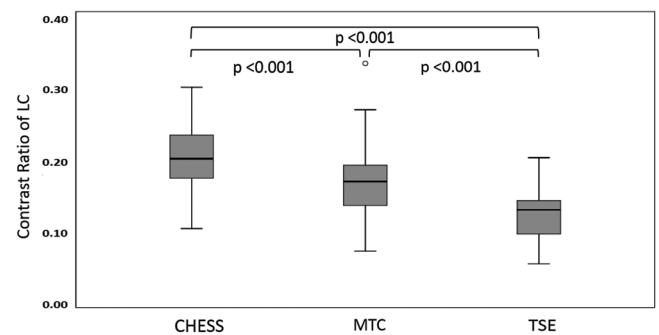

Fig. 5 Contrast ratios of the SNc in the CHESS, MTC, and TSE images. One-way ANOVA followed by post-Bonferroni correction. SNc, substantia nigra pars compacta; CHESS, chemical shift selective; MTC, magnetization transfer contrast; TSE, turbo spin-echo; ANOVA, analysis of variance.

Fig. 6 Contrast ratios of the LC in the CHESS, MTC, and TSE images. One-way ANOVA followed by post-Bonferroni correction. LC, locus coeruleus; CHESS, chemical shift selective; MTC, magnetization transfer contrast; TSE, turbo spin-echo; ANOVA, analysis of variance.

Quantitative analysis

The CR_{SN} values of the CHESS, MTC, and TSE images were 0.23 ± 0.03, 0.23 ± 0.04, and 0.19 ± 0.04, respectively. The CR_{SN} values of the CHESS and MTC images were significantly higher than those of the TSE images ($P < 0.001$ and $P < 0.001$, respectively). There were no significant differences between the CHESS and MTC images ($P = 0.78$) (Fig. 5). The CR_{LC} values of the CHESS, MTC, and TSE images were 0.20 ± 0.03, 0.16 ± 0.03, and 0.11 ± 0.02, respectively. The CR_{LC} value of the CHESS images was significantly higher than that of the MTC and TSE images ($P < 0.001$ and $P < 0.001$, respectively), and the CR_{LC} value of the MTC images was significantly higher than that of the TSE images ($P < 0.001$) (Fig. 6).

Discussion

Chemical shift selective and MTC images were superior to TSE images for the visualization of neuromelanin in both the SNc and the LC. The CHESS images were significantly superior, especially for the visualization of the LC. Several studies have investigated the effect of MT by using MTC pulses for neuromelanin imaging; however, no studies have

used a CHESS pulse for the visualization of neuromelanin. The results of our present investigation demonstrated the usefulness of a CHESS pulse in neuromelanin imaging.

Turbo spin-echo sequences are reported to have MT effects because the echo train length containing sequential 180° pulses induces an off-resonance effect that decreases the signal intensity.[17] The slice position is selected by delivering the specific RF pulse at a site that has the same resonance frequency in the gradient magnetic field. In multi-slice imaging, the slice position is changed by shifting the resonance frequency for the RF pulse, which means that off-resonance pulses are exposed in non-selected slices. Thus, multi-slice imaging can have an MT effect. In conventional neuromelanin imaging, the visualization of neuromelanin has been achieved by MT effects in multi-slice imaging with TSE sequences.

In this study, in addition to TSE, an MTC pulse and a CHESS pulse were used for the evaluation. When an MTC pulse is applied, an RF pulse with frequency components distant from the resonant frequency of free water is excited, and the background signal intensity in the brain parenchyma where protein and phospholipids are abundant decreases;[18,19] therefore, an MTC pulse is useful for the visualization of

neuromelanin as reported.[2,14] In the present study, we newly used a CHESS pulse, which is the fat-suppression pulse most frequently used in practice. This method selectively suppresses signals through the saturation of fat signals by applying a prepulse tuned to the resonant frequency of fat, utilizing the difference in the resonant frequency between fat and water protons (3.5 ppm).[4–6] Like MTC, the CHESS method consists of an RF pulse and is expected to have an MT effect.[3] It has been speculated that another reason for the decrease in background signal is that the application of the fat suppression pulse leads to a decrease in signals for lipids in the myelin content of the brain.[20]

Our present findings revealed a difference in visualization between the SNc and LC, with CHESS being superior for the visualization of the LC compared with the SNc. We speculate that this is due to the differences in the molecular structure of neuromelanin between the SNc and LC. Melanin has a high affinity for metal ions. Enochs et al.[21] estimated the T_1 relaxation of each paramagnetic metal ion *in vitro* under the conditions of 20 MHz and 35°C as follows: 7.9/s for Fe^{3+}, 1.6/s for Mn^{2+}, and 0.3/s for Cu^{2+}. This shows that each paramagnetic metal ion enhances the T_1 relaxation effect. Zecca et al.[22] reported that the iron content in the neuromelanin of the LC was 7.9% of that in the neuromelanin of SNc, indicating that the iron content of the LC was much lower than that of the SNc. In addition, the copper content of the LC was higher than that of the SNc. The reason for the slight difference in visualizations between the substantia nigra and the LC was speculated to be due to such differences in molecular structure.[23,24]

Ogisu et al.[2] reported the use of 3D-GRE to improve the signal uniformity and the resolution in the slice direction. However, 3D-GRE does not have an MT effect as TSE has, and thus, an MTC pulse must be applied. The addition of an MTC pulse to 3T-MRI leads to an increased SAR, and this is prominent in 3D-GRE. To avoid the problem of an increased SAR, the repetition time must be extended, which involves an increased scan time. If an MTC pulse is added to 3D-GRE, the scan time would be extended for 60 s. Therefore, in this study, we used 2D imaging, considering that a shorter imaging time is usually required in daily clinical practice. In addition, it is often difficult for patients undergoing neuromelanin imaging to keep still during the imaging procedure, due to conditions such as Parkinson's disease, and a longer scan time may reduce the quality of the images.

This study has some limitations. It was conducted with the aim to reduce the scan time, and the resolution in the direction of slicing as well as the in-plain resolution may have been insufficient. In addition, there was a slice gap due to the use of 2D imaging, and the accurate measurement of the volume of neuromelanin was difficult due to the inhomogeneous B_1 field. However, we believe that the present technique allows clinicians to obtain useful information within a time frame of 3 min 30 s, which is usually feasible in daily clinical practice.

Conclusion

We propose a method of neuromelanin imaging that obtains images within a short time with the use of CHESS.

Conflicts of Interest

The authors declare that they have no conflicts of interest.

References

1. Sasaki M, Shibata E, Tohyama K, et al. Neuromelanin magnetic resonance imaging of locus ceruleus and substantia nigra in Parkinson's disease. Neuroreport 2006; 17:1215–1218.
2. Ogisu K, Kudo K, Sasaki M, et al. 3D neuromelanin-sensitive magnetic resonance imaging with semi-automated volume measurement of the substantia nigra pars compacta for diagnosis of Parkinson's disease. Neuroradiology 2013; 55:719–724.
3. Shin W, Gu H, Yang Y. Incidental magnetization transfer contrast by fat saturation preparation pulses in multislice Look-Locker echo planar imaging. Magn Reson Med 2009; 62:520–526.
4. Haase A, Frahm J, Hänicke W, Matthaei D. 1H NMR chemical shift selective (CHESS) imaging. Phys Med Biol 1985; 30:341–344.
5. Del Grande F, Santini F, Herzka DA, et al. Fat-suppression techniques for 3-T MR imaging of the musculoskeletal system. Radiographics 2014; 34:217–233.
6. Bley TA, Wieben O, François CJ, Brittain JH, Reeder SB. Fat and water magnetic resonance imaging. J Magn Reson Imaging 2010; 31:4–18.
7. Grover VP, Tognarelli JM, Crossey MM, Cox IJ, Taylor-Robinson SD, McPhail MJ. Magnetic resonance imaging: principles and techniques: lessons for clinicians. J Clin Exp Hepatol 2015; 5:246–255.
8. Jin L, Wang J, Wang C, et al. Combined visualization of nigrosome-1 and neuromelanin in the substantia nigra using 3T MRI for the differential diagnosis of essential tremor and de novo Parkinson's disease. Front Neurol 2019; 10:100.
9. Isaias IU, Trujillo P, Summers P, et al. Neuromelanin imaging and dopaminergic loss in Parkinson's disease. Front Aging Neurosci 2016; 8:196.
10. Pyatigorskaya N, Magnin B, Mongin M, et al. Comparative study of MRI biomarkers in the substantia nigra to discriminate idiopathic Parkinson disease. AJNR Am J Neuroradiol 2018; 39:1460–1467.
11. Kashihara K, Shinya T, Higaki F. Neuromelanin magnetic resonance imaging of nigral volume loss in patients with Parkinson's disease. J Clin Neurosci 2011; 18:1093–1096.
12. Matsuura K, Maeda M, Yata K, et al. Neuromelanin magnetic resonance imaging in Parkinson's disease and multiple system atrophy. Eur Neurol 2013; 70:70–77.
13. Reimão S, Pita Lobo P, Neutel D, et al. Quantitative analysis versus visual assessment of neuromelanin MR imaging for the diagnosis of Parkinson's disease. J Parkinsons Dis 2015; 5:561–567.

14. Chen X, Huddleston DE, Langley J, et al. Simultaneous imaging of locus coeruleus and substantia nigra with a quantitative neuromelanin MRI approach. Magn Reson Imaging 2014; 32:1301–1306.
15. Shibata E, Sasaki M, Tohyama K, et al. Age-related changes in locus ceruleus on neuromelanin magnetic resonance imaging at 3 Tesla. Magn Reson Med Sci 2006; 5:197–200.
16. Takahashi J, Shibata T, Sasaki M, et al. Detection of changes in the locus coeruleus in patients with mild cognitive impairment and Alzheimer's disease: high-resolution fast spin-echo T1-weighted imaging. Geriatr Gerontol Int 2015; 15:334–340.
17. Santyr GE. Magnetization transfer effects in multislice MR imaging. Magn Reson Imaging 1993; 11:521–532.
18. Mehta RC, Pike GB, Enzmann DR. Magnetization transfer MR of the normal adult brain. AJNR Am J Neuroradiol 1995; 16:2085–2091.
19. Knauth M, Forsting M, Hartmann M, Heiland S, Balzer T, Sartor K. MR enhancement of brain lesions: increased contrast dose compared with magnetization transfer. AJNR Am J Neuroradiol 1996; 17:1853–1859.
20. O'Brien JS, Sampson EL. Lipid composition of the normal human brain: gray matter, white matter, and myelin. J Lipid Res 1965; 6:537–544.
21. Enochs WS, Hyslop WB, Bennett HF, Brown RD, Koenig SH, Swartz HM. Sources of the increased longitudinal relaxation rates observed in melanotic melanoma. An in vitro study of synthetic melanins. Invest Radiol 1989; 24:794–804.
22. Zecca L, Stroppolo A, Gatti A, et al. The role of iron and copper molecules in the neuronal vulnerability of locus coeruleus and substantia nigra during aging. Proc Natl Acad Sci USA 2004; 101:9843–9848.
23. Sulzer D, Cassidy C, Horga G, et al. Neuromelanin detection by magnetic resonance imaging (MRI) and its promise as a biomarker for Parkinson's disease. NPJ Parkinsons Dis 2018; 4:11.
24. Enochs WS, Petherick P, Bogdanova A, Mohr U, Weissleder R. Paramagnetic metal scavenging by melanin: MR imaging. Radiology 1997; 204:417–423.